Proteomics Analysis Identifies Phosphorylation-dependent α-Synuclein Protein Interactions*

Melinda A. McFarland‡§, Christopher E. Ellis§¶, Sanford P. Markey‡, and Robert L. Nussbaum‖**

Mutations and copy number variation in the *SNCA* gene encoding the neuronal protein α-synuclein have been linked to familial Parkinson disease (Thomas, B., and Beal, M. F. (2007) Parkinson's disease. *Hum. Mol. Genet.* 16, R183–R194). The carboxyl terminus of α-synuclein can be phosphorylated at tyrosine 125 and serine 129, although only a small fraction of the protein is phosphorylated under normal conditions (Okochi, M., Walter, J., Koyama, A., Nakajo, S., Baba, M., Iwatsubo, T., Meijer, L., Kahle, P. J., and Haass, C. (2000) Constitutive phosphorylation of the Parkinson's disease associated α-synuclein. *J. Biol. Chem.* 275, 390–397). Under pathological conditions, such as in Parkinson disease, α-synuclein is a major component of Lewy bodies, a pathological hallmark of Parkinson disease, and is mostly phosphorylated at Ser-129 (Anderson, J. P., Walker, D. E., Goldstein, J. M., de Laat, R., Banducci, K., Caccavello, R. J., Barbour, R., Huang, J. P., Kling, K., Lee, M., Diep, L., Keim, P. S., Shen, X. F., Chataway, T., Schlossmacher, M. G., Seubert, P., Schenk, D., Sinha, S., Gai, W. P., and Chilcote, T. J. (2006) Phosphorylation of Ser-129 is the dominant pathological modification of α-synuclein in familial and sporadic Lewy body disease. *J. Biol. Chem.* 281, 29739–29752). Controversy exists over the extent to which phosphorylation of α-synuclein and/or the visible protein aggregation in Lewy bodies are steps in disease pathogenesis, are protective, or are neutral markers for the disease process. Here we used the combination of peptide pulldown assays and mass spectrometry to identify and compare protein-protein interactions of phosphorylated and non-phosphorylated α-synuclein. We showed that non-phosphorylated α-synuclein carboxyl terminus pulled down protein complexes that were highly enriched for mitochondrial electron transport proteins, whereas α-synuclein carboxyl terminus phosphorylated on either Ser-129 or Tyr-125 did not. Instead the set of proteins pulled down by phosphorylated α-synuclein was highly enriched in certain cytoskeletal proteins, in vesicular trafficking proteins, and in a small number of enzymes involved in protein serine phosphorylation. This targeted comparative proteomics approach for unbiased identification of protein-protein interactions suggests that there are functional consequences when α-synuclein is phosphorylated. *Molecular & Cellular Proteomics 7:2123–2137, 2008.*

α-Synuclein is a 140-amino acid protein that is highly expressed in the brain and localizes at presynaptic terminals (1). The protein is associated with several neurodegenerative diseases, and mutations and copy number variants in the gene coding for α-synuclein have been linked to familial Parkinson disease (PD)[1] (2, 44). The presence of large amounts of α-synuclein in the insoluble aggregates known as Lewy bodies, a pathological hallmark of all PD including sporadic disease, also suggests a connection between the protein and disease.

The protein is predominantly natively unfolded in solution but can bind to phospholipid membranes by adopting an amphipathic helical conformation in its amino-terminal 100 amino acids (3). The remainder of the protein, an acidic, hydrophilic 40-amino acid carboxyl-terminal tail, is thought unlikely to participate directly in membrane binding. A physiological role for vesicle binding by α-synuclein is suggested by the observation that in PC12 and chromaffin cells α-synuclein appears to be a negative regulator of synaptic vesicle exocytosis and neurotransmitter release (4). In addition, loss of α-synuclein in cell culture or in mice results in a significant decrease in the population of presynaptic vesicles in the resting or reserve pool (5–7). Further support for a role of α-synuclein in vesicular trafficking comes from modifier screens in *Caenorhabditis elegans* showing that the toxicity that arises from expression of α-synuclein may be modified by proteins involved in vesicle trafficking (8, 9).

The carboxyl-terminal portion of α-synuclein can be phosphorylated at tyrosine at position 125 (Tyr-125) and at serine at position 129 (Ser-129) by Src family kinases and various casein

From the ‡National Institute of Mental Health and ¶NHGRI, National Institutes of Health, Bethesda, Maryland 20891 and the ‖Department of Medicine, Division of Medical Genetics, University of California, San Francisco, California 94143

Received, March 17, 2008, and in revised form, June 26, 2008

Published, MCP Papers in Press, July 9, 2008, DOI 10.1074/mcp.M800116-MCP200

[1] The abbreviations used are: PD, Parkinson disease; NP, peptide consisting of carboxyl-terminal 40 amino acids of α-synuclein; pS129, peptide consisting of carboxyl-terminal 40 amino acids of α-synuclein that is phosphorylated at serine position 129; pY125, peptide consisting of carboxyl-terminal 40 amino acids of α-synuclein that is phosphorylated at tyrosine position 125; VDAC, voltage-dependent anion-selective channel; MAP, microtubule-associated protein; AP-2, adaptor protein complex 2; CaM, calmodulin.

kinases, respectively (10–12). α-Synuclein phosphorylated at Ser-129 is the predominant form of α-synuclein in Lewy bodies but constitutes only a very small fraction of soluble α-synuclein in the neuron (13, 14). There is, however, controversy over the extent to which phosphorylation of α-synuclein at Ser-129 is important in the causation of PD. A phosphomimic form of α-synuclein with aspartic acid replacing serine at position 129 (S129D) was shown to enhance the toxicity of α-synuclein in a *Drosophila* model for PD (15). In contrast, overexpression of S129D α-synuclein using adeno-associated virus injected directly into rat brains appeared relatively non-toxic, whereas the non-phosphorylatable version, with alanine replacing serine 129, was highly neurotoxic (16). Thus, identification of protein-protein interactions of α-synuclein that depend on the phosphorylation state of α-synuclein at Ser-129 or Tyr-125 is likely to shed light on the normal physiological function of α-synuclein phosphorylation as well as identify potential pathways for Lewy body formation and α-synuclein toxicity.

We hypothesized that the hydrophilic tail of α-synuclein constitutes a domain that participates in phosphorylation state-dependent protein-protein interactions intrinsic to the normal function of α-synuclein. Mass spectrometric analysis of protein-protein interactions offers a uniquely unbiased tool for elucidating the components of protein complexes. We decided, therefore, to undertake a mass spectrometric analysis of synaptosomal protein complexes that could be pulled down *in vitro* with a peptide containing the hydrophilic domain comprising the carboxyl-terminal 40 amino acids of α-synuclein. We used a targeted mass spectrometry-based functional proteomics approach to identify qualitative and relative quantitative differences in protein-protein interactions of phosphorylated *versus* non-phosphorylated α-synuclein. We showed that a phosphorylated peptide containing the carboxyl-terminal 40 amino acids of α-synuclein interacted preferentially with cytoskeletal proteins, vesicular trafficking proteins involved in endocytosis, and enzymes involved in protein serine phosphorylation, whereas the non-phosphorylated peptide interacted preferentially with mitochondrial electron transport chain complexes. This suggests that phosphorylation likely has a profound effect on the function and/or localization of α-synuclein.

EXPERIMENTAL PROCEDURES

Peptide Pulldowns—All animal work was done according to protocols reviewed and approved by the NHGRI Animal Care and Use Committee. Mouse brain synaptosomes were isolated as described previously (17) and frozen at −80 °C. For human brain extract fresh normal cortical tissue from human brain was obtained by surgical removal from a single epilepsy patient, embedded in optimum cutting temperature compound, snap frozen in dry ice/isopentane, and stored at −80 °C. The optimum cutting temperature compound was then removed from the tissue at −15 °C in a Leica CM1900 cryostat by surgical dissection, and human synaptosomes were isolated and stored at −80 °C as described previously (17). Protein was quantified using the BCA assay with BSA as a standard (Pierce). The protocol for surgical sample collection (02-N-0014, Research Study of Specimens Obtained during Epilepsy Surgery) was approved by the NINDS Intramural Institutional Review Board. For both preparations, synaptosomes were solubilized in a Triton buffer (~1.5% Triton, 50 mM Tris-HCl (pH 7.4), 100 mM NaCl, 2 mM EGTA, 50 mM NaF, 0.5 mM sodium vanadate, 1× protease inhibitor mixture (Sigma-Aldrich)) resulting in final concentrations of 1% Triton and ~5 mg/ml synaptosome protein and centrifuged at 16,000 × *g* for 10 min at 4 °C, and the supernatant was used for binding experiments.

TABLE I
Biotinylated peptides used for pulldown experiments
Phosphorylated residues in pS129 and pY125 are shown in bold.

NP	GKNEEGAPQEGILEDMPVDPDNEAYEMPSEEGYQDYEPEA
pS129	GKNEEGAPQEGILEDMPVDPDNEAYEMP**S**^{PO4}EEGYQDYEPEA
pY125	GKNEEGAPQEGILEDMPVDPDNEA**Y**^{PO4}EMPSEEGYQDYEPEA
Scrambled	AGEKPNEEYEGDAQPYQGEEGEILSEPDMEMPYVAEDPND

Bait peptides consisted of amino-terminally tagged biotinylated peptides (Quality Controlled Biochemicals, Hopkinton, MA) (Table I). The peptides used were as follows: the non-phosphorylated carboxyl-terminal 40 amino acids of human α-synuclein (NP); carboxyl-terminal 40-amino acid peptides phosphorylated either at Ser-129 (pS129) or at Tyr-125 (pY125), respectively; and a scrambled control peptide with the same amino acid content as NP but with the residues in random order. Peptides were quantified by absorbance using a Beckman DU640 spectrophotometer (260 nm) and calculated using the molar extinction coefficient of each peptide or by the BCA assay with BSA as a standard (Pierce).

For binding incubations, 400 μl of streptavidin-coated Dynabeads (Dynal, Carlsbad, CA) were incubated at 4 °C overnight in binding/wash buffer (50 mM Tris-HCl (pH 7.4), 100 mM NaCl, 2 mM EGTA, 50 mM NaF, 0.5 mM sodium vanadate, 1× protease inhibitor mixture (Sigma)) with ~1.5 mg of solubilized mouse brain synaptosome protein and 4 nmol of biotinylated peptide. Final binding conditions contained ~0.15% Triton and ~800 mg/ml synaptosome protein. Samples were washed three times in binding/wash buffer, and proteins were eluted in SDS loading buffer (50 mM Tris-HCl (pH 6.8), 2% SDS, 10% glycerol, 0.1% bromphenol blue) by heating at 65 °C for 5 min. Binding incubations for each peptide were performed in duplicate and combined prior to elution. The eluted proteins were then heated at 95 °C for 5 min and separated by SDS-PAGE (4–20%) (Invitrogen), and the gel was stained with GelCode Blue (Pierce). All pulldowns and subsequent mass spectrometric analysis were repeated three times from three different pooled lysates.

In-gel Digestion—Each gel lane was manually excised top to bottom into 40 ~ 2-mm bands. In-gel tryptic digestion and peptide extraction followed a modified version of a standard protocol (18). Briefly individual gel bands were destained with 50% methanol in 100 mM ammonium bicarbonate, dehydrated with 50% acetonitrile followed by 100% acetonitrile, and dried. Samples were reduced and alkylated with 45 mM DTT at 60 °C followed by 100 mM iodoacetamide at room temperature. Bands were again dehydrated with 50% acetonitrile followed by 100% acetonitrile and then were rehydrated with 200 ng of sequencing grade trypsin (Promega, Madison, WI) in 25 mM ammonium bicarbonate. Digestion was allowed to proceed overnight at room temperature. Peptides were extracted from the gel pieces with 30% acetonitrile, 1% formic acid and sonicated. Extraction was repeated with 70% acetonitrile, 1% formic acid, and supernatants were pooled and dried prior to analysis.

Mass Spectrometry—For one-dimensional LC-MS/MS samples were resuspended in 5% acetonitrile, 0.1% formic acid and injected into a series LC-VP HPLC system (Shimadzu, Columbia, MD) coupled to an ESI-LCQ Classic ion trap mass spectrometer (Thermo Electron, San Jose, CA). Samples were loaded onto a 75-μm PicoFrit Beta-Basic C_{18} column (New Objectives, Woburn, MA). A linear separation

gradient was developed from 10 to 60% B over 45 min (A, 5% ACN, 95% water, 0.1% formic acid; B, 80% ACN, 20% water, 0.1% formic acid). The chromatographic effluent was introduced at a flow rate of 400 nl/min (19). The LCQ was operated in positive ion mode, and spectra were acquired for 60 min in a data-dependent manner with the top three most intense ions in the MS survey scan selected for MS/MS by CID. Precursor ions selected three times were excluded for 60 s. Peak lists were extracted with Thermo Electron Excalibur 2.0 extract_msn utility without smoothing or signal-to-noise thresholding.

Informatics—The resulting mass spectral peak lists were searched with the Mascot search engine (v.2.1.04; Matrix Sciences, London, UK) against the merged UniProtKB Swiss-Prot and TrEMBL protein sequence library (SPTremb_091706.fas). Search parameters were as follows: *Rodentia* species, trypsin specificity, one allowed missed cleavage, carbamidomethylation fixed modification, methionine oxidation variable modification, precursor ion mass tolerance of 2.0 Da, and fragment ion mass tolerance of ±0.8 Da.

Pulldown assays were replicated with three different lysates resulting in three gels of four lanes each for MS/MS analysis. The tryptic digests of each of the 40 segments were analyzed by LC/MS/MS, resulting in ~75,000 MS/MS spectra per lane when the files from all gel segments were concatenated. Only assigned probable peptide sequences with Mascot Ion Scores exceeding their Identity Scores were used throughout this study to produce minimal, parsimonious protein lists concatenated for each full gel lane. All results from a given pulldown experiment are the pooled data from triplicate gel lanes facilitated by the in-house software MassSieve (20) and DBParser 3.0 (21–23). DBParser 3.0 and MassSieve were also used for peptide and protein level parsimony comparisons across multiple experiments. Additionally individual peptides were culled prior to parsimony analysis if they were only observed once across all experiments.

Label-free relative quantification was determined by two methods. In the first method, differentiation was based on the total peptide "hits" or observations per protein (total number of independent spectra assigned by Mascot to peptides from a given protein and with Ion Scores greater than Identity). Each experiment was normalized relative to total peptide hits for a given bait (24, 25). The number of hits per peptide was distilled by MassSieve to generate the integral of the total number of observations of peptides from a given protein (20). Differences in the affinity of a bait peptide complex for a given protein were calculated as the ratio of normalized peptide hits of one α-synuclein form relative to another.

In the second quantification method, an integral of ion current intensities of the peptide parent ion was calculated by DBParser 3.0 from analysis of primary mass spectrometric survey scans. In brief, extracted ion chromatograms were generated from mass spectrometric raw data, and the integral areas were determined for peptides associated with Mascot peptide assignments identified with Ion Scores greater than Identity (21–23). Summed maximum ion intensities for all peptides mapped to respective proteins were normalized to the total assigned ion current for each experiment. For both methods corresponding gel migrations could also be used to validate peptide comparisons.

Enrichment of a particular protein in a pulldown with either the phosphorylated or non-phosphorylated bait peptide was assessed using the ratio of normalized peptide hits or normalized ion currents for the peptides of that protein obtained using either the phosphorylated or the non-phosphorylated peptide. Enrichment was arbitrarily defined as a 2-fold greater number of normalized peptide hits or normalized ion currents for the phosphorylated *versus* non-phosphorylated bait peptide or vice versa.

Western Analysis—As an adjunct to mass spectrometric analysis, the gels containing synaptosomal proteins eluted from the washed streptavidin-coated beads were transferred to Hybond-P membrane (Amersham Biosciences), membranes were blocked in 5% nonfat milk, PBS with 0.1% Tween 20, and Western analysis was performed. Antibodies used were: core 1; core 2 complex III; and 39-kDa, 30-kDa (NDUFS3), and 17-kDa (NDUFB6) complex I (mouse monoclonal antibodies from Molecular Probes); adaptin β, clathrin heavy chain, and β-spectrin II (mouse monoclonal antibodies from BD Transduction Laboratories); and VDAC (rabbit polyclonal from Alexis Biochemicals). Proteins were then detected by ECL (Amersham Biosciences) and visualized by autoradiography.

RESULTS

Quantitative Analysis of Proteins Pulled Down with Different α-Synuclein Peptides—We sought to identify protein networks that interact with the carboxyl-terminal domain of α-synuclein in a phosphorylation-dependent manner. The experimental design was to pull down mouse brain synaptosomal proteins using biotinylated peptides representing the carboxyl-terminal portion (residues 101–140) of α-synuclein. The peptides were non-phosphorylated (NP), phosphorylated on serine 129 (pS129), or phosphorylated on tyrosine 125 (pY125). A biotinylated peptide with the same amino acids as the NP peptide but with the sequence scrambled was used as a control for nonspecific binding. The control lane (Fig. 1, *Lane 2*) shows very few visible bands other than contaminating streptavidin and BSA products, indicating minimal nonspecific binding. In contrast, many proteins were present in the NP (Fig. 1, *Lane 3*). The pattern was markedly different from that with the phosphorylated peptides pS129 and pY125 (Fig. 1, *Lanes 5* and *6*), which suggested a change in interaction proteins and justified pursuing the identification of these proteins.

Pulldowns were prepared in three independent replicate experiments. Each group of experimental replicate data was parsed into a single merged experiment and yielded a total number of spectra identified, with a Mascot Ions Score greater than its Identity score, of ~13,000 for NP, 15,900 pS129 spectra, 13,900 pY125 spectra, and 5300 for the control (supplemental Fig. 1).

Relative protein quantification determined using both peptide hits quantification and ion current intensity is shown in Tables II–V. We applied stringent thresholds to decide on the inclusion of proteins. First, comparisons were made across the three independent experimental replicates to establish reproducibility (supplemental Fig. 2). Only proteins identified in more than one gel and with greater than one peptide observation were included in the analysis; peptides observed only once across all experiments were discarded prior to analysis. Second, comparisons were based on proteins identified by 10 or more peptide observations. Third, to be considered specific, a protein had to have peptide hits greater than three times that of the scrambled control. Finally for affinity to be preferential, we required that there be 2 times the number of peptide hits depending on the phosphorylation status of the peptide. Ion current -fold changes were also

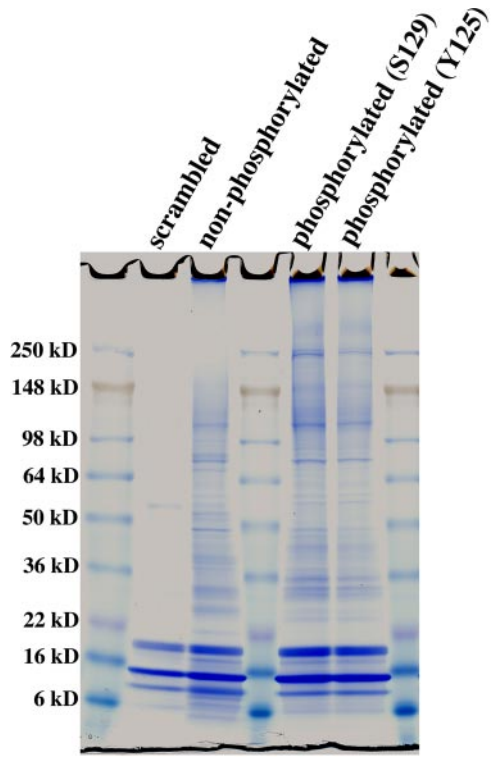

FIG. 1. **Representative SDS-PAGE gel illustrating proteins binding to the carboxyl terminus of α-synuclein in a sequence- and phosphorylation-dependent manner.** Pulldown experiments using biotinylated 40-amino acid peptides that were either scrambled, non-phosphorylated (NP), or phosphorylated on Ser-129 (pS129) or Tyr-125 (pY125) were performed as described under "Experimental Procedures." Each lane is labeled with the peptide (scrambled, NP, pS129, and pY125) that was bound to the magnetic beads and used for each pulldown. Proteins bound to each peptide were eluted and heated at 95 °C for 5 min in Laemmli sample buffer, separated by SDS-PAGE (4–20%), and visualized by GelCode Blue staining. *Lanes 2*, *3*, *5*, and *6* are labeled with the peptide used for the pulldown. Protein markers are in *Lanes 1*, *4*, and *7*.

calculated as an alternative to peptide hit quantification for confirmation of preferential affinity.

There were 85 proteins that showed very significant enrichment (affinity or -fold change) in pulldowns performed with pS129 and pY125 *versus* NP (Table II). These proteins fell into a number of discrete functional groupings. Thirty-nine of these were cytoskeletal proteins, including microtubule-associated protein 1B (MAP1B) previously reported to interact with the carboxyl terminus of α-synuclein (26). Our new finding is the significant enrichment for interaction with MAP1B when α-synuclein was phosphorylated. We also made the novel observation of significant enrichment for a number of presynaptic cytoskeletal elements, particularly the non-erythrocyte αII and βII spectrins (fodrins) along with the known spectrin-binding proteins ankyrin and band 4.1B (27, 28). We also saw significant enrichment for β- and γ-actin (29, 30), non-muscle myosins, and one species of neurofilament. These proteins are present in the presynaptic portion of neurons and form a dense presynaptic cytoskeletal structure known as the presynaptic particle web (31). A second functional group contained six proteins involved in synaptic vesicle endocytosis (32). In particular, we saw the heavy chain of clathrin and the α-1, β-1, and μ subunits of the adaptor protein complex 2 (AP-2) enriched with pS129 and pY125 *versus* NP. A third group of nine proteins enriched in pulldowns with phosphorylated α-synuclein peptide were subunits of enzymes involved in serine/threonine phosphorylation and signaling such as three subunits of calmodulin (CaM) kinase II, the CaM kinase family member MARK2, casein kinase 1, and a serine/threonine-protein phosphatase PP1A. Interestingly casein kinase 2, which is considered to be the kinase primarily responsible for Ser-129 phosphorylation of α-synuclein, was not seen (33). Finally three members of the 14-3-3 family of protein chaperones were enriched in pulldowns using phosphorylated peptides. The interaction between 14-3-3 proteins and α-synuclein has been reported previously, although a preference for phosphorylated α-synuclein was not previously known (34).

When we compared the enrichment for proteins pulled down by pS129 and pY125 *versus* NP, greater enrichment was seen, in nearly every case, with pS129 as compared with the pY125 peptide (Table III). The one exception to this trend was the α subunit of casein kinase 1.

A second class of proteins included those that were preferentially pulled down by NP as compared with pS129 and pY125 (Table IV). The striking finding was that this class of proteins consisted nearly entirely of subunits of the mitochondrial electron transport chain. Of complex I proteins, we observed three of the seven mitochondrially encoded peptides and 28 of 39 nuclearly encoded proteins. We also observed seven of the 11 complex III proteins and eight of 13 complex IV proteins but no complex II proteins. Complexes I, III, and IV, but not complex II, together form a supercomplex, the respirasome (35).

A third major class were proteins pulled down specifically by the carboxyl-terminal portion of α-synuclein as compared with the scrambled control peptide, but the affinity was independent of the phosphorylation status of the bait peptide (Table V). The proteins in this group included microtubule-associated proteins other than MAP1B, *i.e.* MAP1A, MAP2, and MAP4, as well as outer mitochondrial membrane transporters from the solute carrier 25 family and from the porin family of voltage-dependent anion channels. Although no enrichment was seen here, peptides that showed no quantitative differences may require a more targeted approach, such as multiple reaction monitoring analysis, to provide increased accuracy.

Western Blot Confirmation of Quantitative Mass Spectroscopy—We used Western blotting of the mixture of proteins pulled down by phosphorylated and non-phosphorylated peptides as an independent method of assessing the validity of the mass spectrometry results. We chose a subset of five

TABLE II

Proteins with preferential affinity for the Ser-129 phosphorylated α-synuclein interaction network

To be considered specific a protein had to have peptide hits greater than 3 times that of the control. Comparisons are shown only for proteins identified by 10 or more peptide (Pep) hits. A protein was considered to show preferential enrichment if it had 2 times the number of peptide hits in the pS129 pulldown relative to the NP peptide. Ion current -fold changes are also shown as confirmation of peptide hit quantification. n/a, not applicable; Snare, soluble *N*-ethylmaleimide-sensitive factor attachment protein receptors; CNPase, 2′,3′-cyclic-nucleotide 3′-phosphodiesterase.

UniProtKB/Swiss-Prot entry name	Primary accession number	Gene name	Pep hits		pS129 affinity		Unique peptides		Description
			pS129	NP	Normalized Pep hits	Normalized ion current	pS129	NP	
Signaling									
Q6PJ87_MOUSE	Q6PJ87	Csnk1a1	24	0	n/a	n/a	7	0	Casein kinase 1, α1
MARK1_MOUSE	Q8VHJ5	*Mark1*	13	0	n/a	n/a	4	0	Serine/threonine-protein kinase MARK1
Q5RJI5_MOUSE	Q5RJI5	*Brsk1*	11	0	n/a	n/a	2	0	BR serine/threonine kinase 1
KCC2B_MOUSE	P28652	*Camk2b*	185	6	25.2	36.7	7	3	CaM kinase II β chain
Q6PHZ2_MOUSE	Q6PHZ2	*Camk2d*	79	3	21.5	29.8	4	1	CaM kinase II δ chain
Q80TN1_MOUSE	Q80TN1	*Camk2a*	168	13	10.6	25.8	7	4	MKIAA0968 protein (fragment)
MARK2_MOUSE	Q05512	*Mark2*	46	4	9.4		10	1	Serine/threonine-protein kinase MARK2
PP1A_MOUSE	P62137	*Ppp1ca*	16	2	6.5	8.5	3	2	Serine/threonine-protein phosphatase PP1-α catalytic
Cytoskeleton									
Q8C8R3_MOUSE	Q8C8R3	*Ank2*	73	0	n/a	n/a	13	0	Similar to Ankyrin-2
Q6PCN2_MOUSE	Q6PCN2	*Ank2*	48	0	n/a	n/a	11	0	Ankyrin 2, brain
AINX_MOUSE	P46660	*Ina*	40	0	n/a	n/a	9	0	α-Internexin
MYO5A_MOUSE	Q99104	*Myo5a*	28	0	n/a	n/a	6	0	Myosin-5A
Q3UMG4_MOUSE	Q3UMG4	*Ina*	22	0	n/a	n/a	5	0	Internexin neuronal intermediate filament protein
Q3THE2_MOUSE	Q3THE2	*Mylc2b*	22	0	n/a	n/a	5	0	Myosin regulatory light chain
BCAS1_MOUSE	Q80YN3	*Bcas1*	14	0	n/a	n/a	1	0	Novel amplified in breast cancer 1 homolog
CTNB1_MOUSE	Q02248	*Ctnnb1*	13	0	n/a	n/a	6	0	β-Catenin
DYL1_MOUSE	P63168	*Dynll1*	12	0	n/a	n/a	1	0	Dynein light chain 1
Q3TY37_MOUSE	Q3TY37	*Ctnna2*	10	0	n/a	n/a	5	0	Catenin α2
SPTA2_MOUSE	P16546	*Spna2*	256	4	52.3	298.1	33	3	Spectrin α chain, brain
MYH10_MOUSE	Q61879	*Myh10*	48	1	39.2	398.8	14	1	Myosin-10 (myosin heavy chain, non-muscle IIb)
Q3V1V5_MOUSE	Q3V1V5	*Spna2*	143	3	38.9	98.8	18	2	Spectrin α chain, brain
NFL_MOUSE	P08551	*Nefl*	37	1	30.2	217.8	9	1	Neurofilament triplet L protein
TRIM3_MOUSE	Q9R1R2	*Trim3*	33	1	26.9	134.4	7	1	Tripartite motif-containing protein 3
CAZA2_MOUSE	P47754	*Capza2*	34	2	13.9	112.3	6	1	F-actin capping protein α-2 subunit
DCTN2_MOUSE	Q99KJ8	*Dctn2*	16	1	13.1	47.8	5	1	Dynactin subunit 2
MLP3A_MOUSE	Q91VR7	*Map1lc3a*	16	1	13.1	10.8	2	1	Microtubule-associated proteins 1A/1B light chain 3A
SPTB2_MOUSE	Q62261	*Spnb2*	341	22	12.7	64.4	55	15	Spectrin β chain, brain 1
Q80UE4_MOUSE	Q80UE4	*Epb41l2*	26	2	10.6	36.7	7	2	Protein 4.1G
TMOD2_MOUSE	Q9JKK7	*Tmod2*	11	1	9.0	40.8	5	1	Tropomodulin-2
E41L3_MOUSE	Q9WV92	*Epb41l3*	75	8	7.7	17.3	11	5	Band 4.1-like protein 3
ACTB_MOUSE	P60710	*Actb*	182	21	7.1	31.1	15	5	Actin, cytoplasmic 1 (β-actin)
Q9QZ83_MOUSE	Q9QZ83	*Actg1*	173	21	6.7	30.5	13	5	γ-Actin-like protein
Q7TSJ2_MOUSE	Q7TSJ2	*Mtap6*	62	10	5.1	10.7	4	2	Microtubule-associated protein 6
MAP1B_MOUSE	P14873	*Mtap1b*	992	165	4.9	9.2	45	25	Microtubule-associated protein 1B
TBB6_MOUSE	Q922F4	*Tubb6*	51	9	4.6	15.3	5	4	Tubulin β-6 chain
DYL2_MOUSE	Q9D0M5	*Dynll2*	22	4	4.5	32.3	2	1	Dynein light chain 2
P25A_MOUSE	Q7TQD2	*Tppp*	11	2	4.5	8.6	2	1	Tubulin polymerization-promoting protein (TPPP)
Q80Y54_MOUSE	Q80Y54	*Tubb4*	100	29	2.8	15.3	12	10	Tubulin β-4
TBB5_MOUSE	P99024	*Tubb5*	123	36	2.8	14.9	12	10	Tubulin β-5 chain
TBB3_MOUSE	Q9ERD7	*Tubb3*	99	29	2.8	11.4	8	7	Tubulin β-3 chain

TABLE II—*continued*

UniProtKB/Swiss-Prot entry name	Primary accession number	Gene name	Pep hits		pS129 affinity		Unique peptides		Description
			pS129	NP	Normalized Pep hits	Normalized ion current	pS129	NP	
TBA4_MOUSE	P68368	Tuba4	131	43	2.5	11.6	9	7	Tubulin α-4 chain
ACTY_MOUSE	Q8R5C5	*Actr1b*	33	11	2.4	2.5	6	3	β-Centractin
ACTZ_MOUSE	P61164	*Actr1a*	30	10	2.4	2.2	6	2	α-Centractin
Endocytosis									
AP1B1_MOUSE	O35643	*Ap1b1*	26	0	n/a	n/a	6	0	AP-1 complex subunit β-1
AP2M1_MOUSE	P84091	*Ap2m1*	26	1	21.2	48.2	5	1	AP-2 complex subunit μ-1
AP2B1_MOUSE	Q9DBG3	*Ap2b1*	82	8	8.4	20.3	15	4	AP-2 complex subunit β-1
AP2A1_MOUSE	P17426	*Ap2a1*	89	15	4.8	25.5	14	4	AP-2 complex subunit α-1
CLH_MOUSE	Q68FD5	*Cltc*	105	25	3.4	8.5	26	13	Clathrin heavy chain
14-3-3 chaperones									
1433E_MOUSE	P62259	*Ywhae*	24	0	n/a	n/a	4	0	14-3-3 protein ε
1433Z_MOUSE	P63101	*Ywhaz*	26	1	21.2	103.8	5	1	14-3-3 protein ζ/δ
1433G_MOUSE	P61982	*Ywhag*	23	2	9.4	28.5	4	1	14-3-3 protein γ
Neural adhesion molecule									
NTRI_MOUSE	Q99PJ0	*Hnt*	33	2	13.5	185.3	4	1	Neurotrimin precursor
CNTN1_MOUSE	P12960	*Cntn1*	78	16	4.0	13.2	18	7	Contactin-1 precursor
Glutamate transport membrane									
EAA1_MOUSE	P56564	*Slc1a3*	132	38	2.8	4.0	3	2	Excitatory amino acid transporter 1
Snare complex									
SNIP_MOUSE	Q9QWI6	*P140*	15	5	2.4	17.4	4	2	SNAP-25-interacting protein
Mitochondrial proteins									
Q8JZU2_MOUSE	Q8JZU2	*Slc25a1*	13	2	5.3	4.6	3	1	Solute carrier family 25
GHC1_MOUSE	Q9D6M3	*Slc25a22*	10	4	2.0	5.8	5	4	Solute carrier family 25 member 22
LACTB_MOUSE	Q9EP89	*Lactb*	72	0	n/a	n/a	9	0	Serine β-lactamase-like protein LACTB
TFAM_MOUSE	P40630	*Tfam*	15	0	n/a	n/a	3	0	Transcription factor A, mitochondrial precursor
ATPase									
VA0D_MOUSE	P51863	*Atp6v0d1*	29	6	3.9	2.6	6	3	Vacuolar ATP synthase subunit d
Q8CHX2_MOUSE	Q8CHX2	*Atp6v1a*	53	13	3.3	3.7	10	6	Vacuolar ATP synthase catalytic subunit A
G proteins									
GBB1_MOUSE	P62874	*Gnb1*	67	21	2.6	3.8	6	5	Transducin β chain 1
GBB2_MOUSE	P62880	*Gnb2*	43	16	2.2	3.4	6	4	Transducin β chain 2
Ribosomal proteins									
RS7_MOUSE	P62082	*Rps7*	69	26	2.2	6.6	8	6	40 S ribosomal protein S7
RS10_MOUSE	P63325	*Rps10*	11	4	2.2	2.2	2	2	40 S ribosomal protein S10
Miscellaneous									
LSAMP_MOUSE	Q8BLK3	*Lsamp*	20	0	n/a	n/a	5	0	Limbic system-associated membrane protein precursor
CALM_MOUSE	P62204	*Calm3*	16	0	n/a	n/a	3	0	CaM
Q6DFY2_MOUSE	Q6DFY2	*Opcml*	14	0	n/a	n/a	3	0	Opioid-binding protein/cell adhesion molecule-like
ROA2_MOUSE	O88569	*Hnrpa2b1*	10	0	n/a	n/a	1	0	Heterogeneous nuclear ribonucleoproteins A2/B1
H2A2B_MOUSE	Q64522	*Hist2h2ab*	11	1	9.0	40.0	3	1	Histone H2A type 2-B
CN37_MOUSE	P16330	*Cnp1*	74	7	8.6	12.3	7	4	CNPase
CSKI1_MOUSE	Q6P9K8	*Caskin1*	49	5	8.0	13.6	7	2	CASK-interacting protein 1
CENG1_MOUSE	Q3UHD9	*Centg1*	155	17	7.4	21.6	14	5	Centaurin-γ 1
USMG5_MOUSE	Q78IK2	*Usmg5*	10	2	4.1	21.4	2	1	Up-regulated during skeletal muscle growth protein 5
THY1_MOUSE	P01831	*Thy1*	58	14	3.4	7.8	5	2	Thy-1 membrane glycoprotein precursor
ALDOA_MOUSE	P05064	*Aldoa*	117	37	2.6	4.8	8	7	Fructose-bisphosphate aldolase A
SYPH_MOUSE	Q62277	*Syp*	11	4	2.2	5.6	2	1	Synaptophysin

TABLE III

Protein interactions with a phosphorylation site preference

Preferential enrichment with structural proteins was usually seen with either Ser-129 or Tyr-125 phosphorylation over the NP, although the affinity for the Ser-129 phosphorylated peptide was generally greater than for peptides phosphorylated at Tyr-125. Exceptions are several kinases that were not enriched in pulldowns with the peptide phosphorylated at Tyr-125 and the first protein in the table, casein kinase 1, α1, for which peptide phosphorylated at Tyr-125 showed greater enrichment. CNPase, 2′,3′-cyclic-nucleotide 3′-phosphodiesterase; Pep, peptide.

UniProtKB/Swiss-Prot entry name	Primary accession number	Gene name	Pep hits		pS129 affinity		Unique peptides		Description
			pS129	pY125	Normalized Pep hits	Normalized ion current	pS129	pY125	
pY125 affinity > pS129 affinity									
Q6PJ87_MOUSE	Q6PJ87	Csnk1a1	24	43	0.5	0.5	7	7	Casein kinase 1, α1
pS129 affinity > pY125 affinity									
Signaling									
Q6PHZ2_MOUSE	Q6PHZ2	*Camk2d*	79	24	2.9	1.8	4	4	CaM kinase II δ chain
MARK2_MOUSE	Q05512	*Mark2*	46	16	2.5	n/a	10	7	Serine/threonine-protein kinase MARK2
Q5RJI5_MOUSE	Q5RJI5	*Brsk1*	11	4	2.4	3.4	2	2	BR serine/threonine kinase 1
PP1A_MOUSE	P62137	*Ppp1ca*	16	3	4.7	4.5	3	2	Serine/threonine-protein phosphatase PP1-α catalytic
Cytoskeletal									
Q3V1V5_MOUSE	Q3V1V5	*Spna2*	143	62	2.0	1.7	18	15	Spectrin α chain, brain
MYH10_MOUSE	Q61879	*Myh10*	48	13	3.2	4.0	14	8	Myosin-10 (myosin heavy chain, non-muscle IIb)
AINX_MOUSE	P46660	*Ina*	40	13	2.7	4.4	9	7	α-Internexin
ACTZ_MOUSE	P61164	*Actr1a*	30	11	2.4	5.4	6	2	α-Centractin
Q3THE2_MOUSE	Q3THE2	*Mylc2b*	22	7	2.8	3.0	5	3	Myosin regulatory light chain
Q3UMG4_MOUSE	Q3UMG4	*Ina*	22	7	2.8	4.0	5	3	Internexin neuronal intermediate filament protein
BCAS1_MOUSE	Q80YN3	*Bcas1*	14	1	12.3	8.8	1	1	Novel amplified in breast cancer 1 homolog
TRIM3_MOUSE	Q9R1R2	*Trim3*	33	5	5.8	3.3	7	4	Tripartite motif-containing protein 3
Q3TY37_MOUSE	Q3TY37	*Ctnna2*	10	4	2.2	4.4	5	3	Catenin α2
Mitochondria-related									
Q8JZU2_MOUSE	Q8JZU2	*Slc25a1*	13	5	2.3	2.2	3	2	Solute carrier family 25
LACTB_MOUSE	Q9EP89	*Lactb*	72	2	31.6	138.4	9	1	Serine β-lactamase-like protein LACTB
TFAM_MOUSE	P40630	*Tfam*	15	5	2.6	3.9	3	2	Transcription factor A, mitochondrial precursor
Miscellaneous									
CN37_MOUSE	P16330	*Cnp1*	74	28	2.3	5.8	7	6	CNPase
RS10_MOUSE	P63325	*Rps10*	11	3	3.2	2.8	2	2	40 S ribosomal protein S10
H2A2B_MOUSE	Q64522	*Hist2h2ab*	11	4	2.4	3.4	3	2	Histone H2A type 2-B

TABLE IV

Proteins with preferential affinity for the non-phosphorylated α-synuclein interaction network

Criteria were the same as in Table II. A protein was considered to show preferential affinity if it had 2 times the number of peptide (Pep) hits in the non-phosphorylated pulldown relative to the phosphorylated. n/a, not applicable.

UniProtKB/Swiss-Prot entry name	Primary accession number	Gene name	Pep hits		NP affinity		Unique peptides		Description
			NP	pS129	Normalized Pep hits	Normalized ion current	NP	pS129	
Complex I									
NDUAB_MOUSE	Q9D8B4	*Ndufa11*	28	0	n/a	n/a	3	0	NADH-ubiquinone oxidoreductase subunit B14.7
NU1M_MOUSE	P03888	*ND1*	22	0	n/a	n/a	1	0	NADH-ubiquinone oxidoreductase chain 1
NIPM_MOUSE	Q99LY9	*Ndufs5*	14	0	n/a	n/a	2	0	NADH-ubiquinone oxidoreductase 15-kDa subunit
NU5M_MOUSE	P03921	*ND5*	47	2	28.8	22.9	3	2	NADH-ubiquinone oxidoreductase chain 5
NUBM_MOUSE	Q91YT0	*Ndufv1*	164	14	14.3	28.1	11	5	NADH-ubiquinone oxidoreductase 51-kDa subunit
NDUBB_MOUSE	O09111	*Ndufb11*	35	3	14.3	12.1	5	2	NADH-ubiquinone oxidoreductase ESSS subunit
NUYM_MOUSE	Q9CXZ1	*Ndufs4*	11	1	13.5	10.0	3	1	NADH-ubiquinone oxidoreductase 18-kDa subunit
NDUB3_MOUSE	Q9CQZ6	*Ndufb3*	20	2	12.2	4.9	2	1	NADH-ubiquinone oxidoreductase B12 subunit
NUCM_MOUSE	Q91WD5	*Ndufs2*	167	26	7.9	14.3	14	8	NADH-ubiquinone oxidoreductase 49-kDa subunit
NDUB8_MOUSE	Q9D6J5	*Ndufb8*	12	2	7.3	6.9	3	1	NADH-ubiquinone oxidoreductase ASHI subunit
NUIM_MOUSE	Q8K3J1	*Ndufs8*	71	12	7.2	23.8	6	3	NADH-ubiquinone oxidoreductase 23-kDa subunit
NDUB6_MOUSE	Q3UIU2	*Ndufb6*	23	4	7.0	8.3	2	2	NADH-ubiquinone oxidoreductase B17 subunit
NDUB7_MOUSE	Q9CR61	*Ndufb7*	97	17	7.0	11.5	9	4	NADH-ubiquinone oxidoreductase B18 subunit
NDUAA_MOUSE	Q99LC3	*Ndufa10*	74	13	7.0	18.9	12	6	NADH-ubiquinone oxidoreductase 42-kDa subunit
NUAM_MOUSE	Q91VD9	*Ndufs1*	491	89	6.8	17.1	28	15	NADH-ubiquinone oxidoreductase 75-kDa subunit
NUKM_MOUSE	Q9DC70	*Ndufs7*	69	13	6.5	33.9	6	3	NADH-ubiquinone oxidoreductase 20-kDa subunit
NU2M_MOUSE	P03893	*Mtnd2*	15	3	6.1	8.0	2	1	NADH-ubiquinone oxidoreductase chain 2
N4BM_MOUSE	Q9CQ54	*Ndufc2*	18	4	5.5	15.0	2	1	NADH-ubiquinone oxidoreductase subunit B14.5b
NUHM_MOUSE	Q9D6J6	*Ndufv2*	95	22	5.3	13.3	9	7	NADH-ubiquinone oxidoreductase 24-kDa subunit
NDUB9_MOUSE	Q9CQJ8	*Ndufb9*	73	17	5.3	13.5	3	2	NADH-ubiquinone oxidoreductase B22 subunit
NDUA6_MOUSE	Q9CQZ5	*Ndufa6*	29	7	5.1	15.2	3	1	NADH-ubiquinone oxidoreductase B14 subunit
NDUB5_MOUSE	Q9CQH3	*Ndufb5*	21	6	4.3	15.0	3	2	NADH-ubiquinone oxidoreductase SGDH subunit
Q6GTD3_MOUSE	Q6GTD3	*Ndufa9*	87	25	4.3	7.5	9	6	NADH dehydrogenase (ubiquinone) 1α subcomplex, 9
NU4M_MOUSE	P03911	*ND4*	24	7	4.2	7.8	4	3	NADH-ubiquinone oxidoreductase chain 4
NDUBA_MOUSE	Q9DCS9	*Ndufb10*	131	39	4.1	11.7	7	6	NADH-ubiquinone oxidoreductase PDSW subunit
NDUA5_MOUSE	Q9CPP6	*Ndufa5*	17	6	3.5	5.4	3	2	NADH-ubiquinone oxidoreductase 13-kDa B subunit
NDUAC_MOUSE	Q7TMF3	*Ndufa12*	16	6	3.3	10.0	4	2	NADH-ubiquinone oxidoreductase subunit B17.2
NUGM_MOUSE	Q9DCT2	*Ndufs3*	113	43	3.2	10.7	10	7	NADH-ubiquinone oxidoreductase 30-kDa subunit
NDUAD_MOUSE	Q9ERS2	*Ndufa13*	65	26	3.1	13.8	5	5	NADH-ubiquinone oxidoreductase B16.6 subunit
NDUA8_MOUSE	Q9DCJ5	*Ndufa8*	40	18	2.7	10.8	5	3	NADH-ubiquinone oxidoreductase 19-kDa subunit
NDUB4_MOUSE	Q9CQC7	*Ndufb4*	21	11	2.3	9.1	2	2	NADH-ubiquinone oxidoreductase B15 subunit
Complex III									
UCR6_MOUSE	Q9D855	*Uqcrb*	18	2	11.0	30.6	3	1	Ubiquinol-cytochrome *c* reductase complex 14-kDa protein
UQCR1_MOUSE	Q9CZ13	*Uqcrc1*	289	62	5.7	14.5	14	9	Ubiquinol-cytochrome *c* reductase complex core protein I
CY1_MOUSE	Q9D0M3	*Cyc1*	168	40	5.1	14.5	7	5	Cytochrome c_1, heme protein, mitochondrial precursor
UCRI_MOUSE	Q9CR68	*Uqcrfs1*	118	36	4.0	9.3	8	5	Ubiquinol-cytochrome *c* reductase iron-sulfur subunit
UQCR2_MOUSE	Q9DB77	*Uqcrc2*	215	66	4.0	9.4	15	13	Ubiquinol-cytochrome *c* reductase complex core protein 2
UCR10_MOUSE	Q8R1I1	*Uqcr10*	19	7	3.3	3.6	2	1	Ubiquinol-cytochrome *c* reductase complex 7.2-kDa protein
UCRQ_MOUSE	Q9CQ69	*Uqcrq*	16	7	2.8	8.4	1	1	Ubiquinol-cytochrome *c* reductase complex 9.5-kDa protein
Complex IV									
COX6C_MOUSE	Q9CPQ1	*Cox6c*	20	2	12.2	44.6	2	1	Cytochrome *c* oxidase polypeptide Vic
Q9MD68_MOUSE	Q9MD68	*mt-Co1*	19	3	7.8	8.0	1	1	Cytochrome oxidase subunit 1
COX7R_MOUSE	Q61387	*Cox7a2l*	15	3	6.1	7.3	2	1	Cytochrome *c* oxidase subunit VIIa-related protein

TABLE IV—*continued*

UniProtKB/Swiss-Prot entry name	Primary accession number	Gene name	Pep hits		NP affinity		Unique peptides		Description
			NP	pS129	Normalized Pep hits	Normalized ion current	NP	pS129	
CX7A2_MOUSE	P48771	*Cox7a2*	57	12	5.8	13.1	2	2	Cytochrome *c* oxidase subunit VIIa-L
COX5B_MOUSE	P19536	*Cox5b*	15	4	4.6	12.5	1	1	Cytochrome *c* oxidase polypeptide Vb
COX2_MOUSE	P00405	*COX2*	192	73	3.2	9.3	4	4	Cytochrome *c* oxidase subunit 2
COX5A_MOUSE	P12787	*Cox5a*	28	13	2.6	2.8	3	2	Cytochrome *c* oxidase polypeptide Va
CX6A1_MOUSE	P43024	*Cox6a1*	21	11	2.3	1.6	1	1	Cytochrome *c* oxidase polypeptide VIa
Mitochondrial membrane proteins									
Q3U5Y8_MOUSE	Q3U5Y8	*Fam82c*	18	0	n/a	n/a	4	0	Protein FAM82C
GLPK_MOUSE	Q64516	*Gyk*	10	2	6.1	4.0	2	1	Glycerol kinase
Synaptic vesicle proteins									
VAPA_MOUSE	Q9WV55	*Vapa*	81	17	5.8	21.2	6	3	Vesicle-associated membrane protein-associated protein A
VAPB_MOUSE	Q9QY76	*Vapb*	49	11	5.5	13.5	3	3	Vesicle-associated membrane protein-associated protein B
Mitochondrial transport membrane proteins									
Q3TWD3_MOUSE	Q3TWD3	*Samm50*	25	8	3.8	3.0	10	6	SAM50-like protein CGI-51 homolog
Q3TBZ2_MOUSE	Q3TBZ2	*Tomm40*	16	8	2.4	1.2	4	3	Translocase of outer mitochondrial membrane 40 homolog
Miscellaneous									
STXB1_MOUSE	O08599	*Stxbp1*	111	50	2.7	5.3	17	14	Syntaxin-binding protein 1 (Unc-18-1)

proteins for which robust antibodies were available for Western analysis of brain proteins pulled down by the various peptides. As shown in Fig. 2, we confirmed that all five of the identified proteins showed a similar pattern of enrichment in complexes pulled down by pS129 and pY125 peptides or the NP peptide as we found with the mass spectrometric analysis.

Physiological Relevance for Human Brain—Because these studies were all carried out using human α-synuclein peptides to pull down mouse synaptosomal proteins, we wanted to make sure that the marked differences in affinity of synaptosomal proteins based on the phosphorylation state of the bait peptide was conserved with human synaptosomal proteins. We carried out a Western blot analysis of proteins pulled down by the bait peptides using human brain extracts and found very similar findings with human and mouse brain extracts (Fig. 3).

Finally we asked whether the protein interactions seen with the carboxyl-terminal domain of α-synuclein would be replicated when the domain was part of the full-length protein. Full-length α-synuclein at 3-fold molar excess to NP was able to partially compete the pulldown of three different electron transport chain proteins as well as the mitochondrial VDAC; 10-fold molar excess completely blocked the pulldown (Fig. 4). Because recombinant α-synuclein containing amino acids 1–124 (lacking the last 15 amino acids) failed to compete even when present at 10-fold molar excess, the competition seen with the full-length protein was not a nonspecific effect of adding an excess of recombinant protein or peptide. Although we do not know the minimum extent of the interacting domain, interruption between residues 124 and 125 destroyed the interaction because neither the truncated protein containing residues 1–124 nor a peptide containing the terminal 16 amino acids, including the Ser-129 residue, was able to compete (supplemental Fig. 3). Finally full-length mouse α-synuclein and full-length human β-synuclein were able to compete with biotinylated NP peptide in the pulldown, whereas human γ-synuclein, another α-synuclein paralog, was not (supplemental Fig. 3). Mouse α-synuclein and human β-synuclein are highly homologous to human α-synuclein at their carboxyl termini and undergo phosphorylation on serine (36, 37). In contrast, γ-synuclein has very little homology to α-synuclein at its carboxyl terminus, and, therefore, it is not surprising that it was not able to compete with the NP peptide in our pulldown experiments (37).

DISCUSSION

Our targeted functional proteomics approach provides a broad and unbiased look at the differences in protein networks associated with phosphorylation of α-synuclein. Label-free relative quantification was determined by two methods: the number of independent assignments or hits of a given peptide (more sensitive to minor components) and the ion current intensity (more accurate for major components). Both quantification methods are widely used for initial profiling in

TABLE V

Proteins with no detectable phosphorylation-dependent affinity

These proteins appeared equally in pulldowns with both forms of α-synuclein. Filter criteria were the same as in Table II. Pep, peptide; Snare, soluble *N*-ethylmaleimide-sensitive factor attachment protein receptors.

UniProtKB/Swiss-Prot entry name	Primary accession number	Gene name	Pep hits		pS129 affinity		Unique peptides		Description
			pS129	NP	Normalized Pep hits	Normalized ion current	pS129	NP	
Microtubule-based vesicle mobility									
MAP2_MOUSE	P20357	*Mtap2*	152	85	1.5	4.3	22	14	Microtubule-associated protein 2
Q3UHB7_MOUSE	Q3UHB7	*Map1a*	723	497	1.2	1.9	35	33	Microtubule-associated protein 1 A
MAP1A_MOUSE	Q9QYR6	*Map1a*	625	437	1.2	2.2	20	19	Microtubule-associated protein 1A
Q7TPD4_MOUSE	Q7TPD4	*Mtap4*	53	50	0.9	1.3	6	7	Microtubule-associated protein 4
Q3UIS2_MOUSE	Q3UIS2	*Mtap4*	115	146	0.6	1.0	9	11	Microtubule-associated protein 4
Q8CIL3_MOUSE	Q8CIL3	*Mtap7d1*	17	23	0.6	0.6	2	3	Arginine/proline-rich coiled-coil 1
Mitochondrial carrier membrane proteins									
MPCP_MOUSE	Q8VEM8	*Slc25a3*	28	12	1.9	1.7	7	5	Solute carrier family 25 member 3
MTCH2_MOUSE	Q791V5	*Mtch2*	15	17	0.7	1.3	3	3	Mitochondrial carrier homolog 2
CMC1_MOUSE	Q8BH59	*Slc25a12*	176	206	0.7	1.4	16	19	Solute carrier family 25 member 12
M2OM_MOUSE	Q9CR62	*Slc25a11*	77	95	0.7	0.5	7	7	Solute carrier family 25 member 11
CMC2_MOUSE	Q9QXX4	*Slc25a13*	10	14	0.6	8.3	2	3	Solute carrier family 25 member 13
Heat shock proteins									
GRP75_MOUSE	P38647	*Hspa9a*	27	12	1.8	2.5	9	6	GRP 75 (mortalin)
GRP78_MOUSE	P20029	*Hspa5*	20	9	1.8	2.2	5	1	GRP 78 (BiP)
Mitochondrial membrane proteins									
TOM22_MOUSE	Q9CPQ3	*Tomm22*	18	12	1.2	0.8	4	4	Translocase of outer membrane 22 kDa
VDAC1_MOUSE	Q60932	*Vdac1*	393	333	1.0	0.9	17	17	Voltage-dependent anion-selective channel protein 1
VDAC2_MOUSE	Q60930	*Vdac2*	170	269	0.5	0.8	8	8	Voltage-dependent anion-selective channel protein 2
Q5EBQ0_MOUSE	Q5EBQ0	*Vdac3*	180	288	0.5	0.7	8	8	Voltage-dependent anion channel 3
Voltage-gated potassium channel									
KCAB2_MOUSE	P62482	*Kcnab2*	185	142	1.1	1.6	12	10	Voltage-gated potassium channel subunit β-2
KCAB1_MOUSE	P63143	*Kcnab1*	35	28	1.0	3.3	3	3	Voltage-gated potassium channel subunit β-1
ATP synthase									
ATP5H_MOUSE	Q9DCX2	*Atp5h*	32	13	2.0	3.1	6	4	ATP synthase D chain
ATPG_MOUSE	Q91VR2	*Atp5c1*	137	58	1.9	2.3	4	4	ATP synthase γ chain
AT5F1_MOUSE	Q9CQQ7	*Atp5f1*	27	16	1.4	2.1	4	3	ATP synthase B chain
ATPase									
VATB2_MOUSE	P62814	*Atp6v1b2*	43	22	1.6	2.5	10	9	Vacuolar proton pump B isoform 2
VPP1_MOUSE	Q9Z1G4	*Atp6v0a1*	27	15	1.5	2.3	9	6	Vacuolar proton translocating ATPase 116-kDa subunit a isoform 1
G proteins									
GNAO1_MOUSE	P18872	*Gnao1*	55	32	1.4	2.9	7	4	Guanine nucleotide-binding protein G_o subunit α1
Membrane proteins									
MGST3_MOUSE	Q9CPU4	*Mgst3*	37	35	0.9	1.1	3	2	Microsomal glutathione *S*-transferase 3
IMMT_MOUSE	Q8CAQ8	*Immt*	103	158	0.5		10	12	Mitochondrial inner membrane protein (mitofilin)
Snare complex									
STX1A_MOUSE	O35526	*Stx1a*	30	34	0.7	1.1	6	7	Syntaxin-1A (neuron-specific antigen HPC-1)
Glutamate transport, membrane									
EAA2_MOUSE	P43006	*Slc1a2*	49	42	1.0	0.9	7	4	Sodium-dependent glutamate/aspartate transporter 2
Electron transport chain									
NDUA2_MOUSE	Q9CQ75	*Ndufa2*	8	11	0.6	0.2	1	1	NADH-ubiquinone oxidoreductase B8 subunit
CX6B1_MOUSE	P56391	*Cox6b1*	11	17	0.5	0.1	3	3	Cytochrome *c* oxidase subunit VIb isoform 1

TABLE V—*continued*

UniProtKB/Swiss-Prot entry name	Primary accession number	Gene name	Pep hits		pS129 affinity		Unique peptides		Description
			pS129	NP	Normalized Pep hits	Normalized ion current	pS129	NP	
Miscellaneous									
CD47_MOUSE	Q61735	*Cd47*	18	11	1.3	0.8	3	2	Integrin-associated protein
Q91VC6_MOUSE	Q91VC6	*Glul*	18	11	1.3	3.9	4	4	Glutamine synthetase
SYT2_MOUSE	P46097	*Syt2*	45	30	1.2	2.1	5	3	Synaptotagmin-2
Q2KHL7_MOUSE	Q2KHL7	*Icam5*	58	47	1.0	2.2	8	8	Intercellular adhesion molecule 5, telencephalin
PHB_MOUSE	P67778	*Phb*	36	30	1.0	0.9	8	8	Prohibitin
CHCH3_MOUSE	Q9CRB9	*Chchd3*	21	25	0.7	0.4	3	4	Coiled-coil-helix-coiled-coil-helix domain-containing protein 3
Q6GQU1_MOUSE	Q6GQU1	*Hk1*	97	131	0.6	1.0	16	17	Hk1 protein
PHB2_MOUSE	O35129	*Phb2*	11	15	0.6	1.4	5	5	Prohibitin-2
PDIP3_MOUSE	Q8BG81	*Poldip3*	6	10	0.5	0.7	3	3	Polymerase δ-interacting protein 3

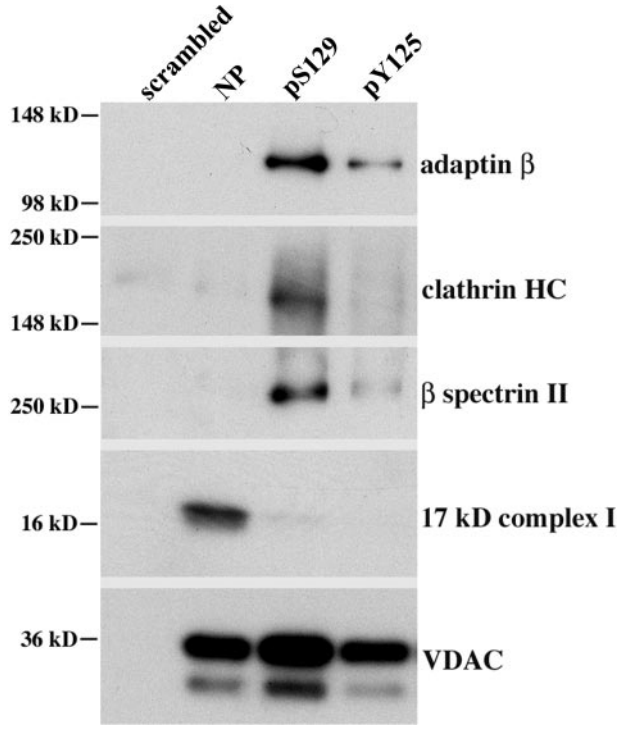

FIG. 2. **Composite of Western analyses confirming phosphorylation-dependent binding of selected mouse proteins.** Pulldown experiments were performed as in Fig. 1. Each lane is labeled with the peptide (scrambled, NP, pS129, and pY125) that was bound to the magnetic beads and used for each pulldown. Eluted proteins bound to each peptide were separated by SDS-PAGE (4–20%), and Western analysis was performed as described under "Experimental Procedures" with various antibodies as indicated to the *right* of the Western blots. *HC*, heavy chain.

high throughput comparative proteomics studies (38, 39). Tables II–IV provide strong evidence to support a change in the role of α-synuclein upon phosphorylation.

Phosphorylated α-Synuclein Affinity—A striking and biologically intriguing observation is the enrichment for cytoskeletal proteins seen with phosphorylated *versus* non-phosphorylated α-synuclein carboxyl-terminal peptide. Structural proteins are frequent contaminants in pulldown assays and proteomics studies. However, we used very strict cutoffs for inclusion and for consideration as relevant preferential interactions. Many more structural proteins did not make our threshold for inclusion and can be found in the supplemental material. Thus, the proteins shown in Tables II–V are shown with confidence.

The interaction of MAP1B with the carboxyl-terminal 45 amino acids of α-synuclein has been observed previously, although an increased affinity with phosphorylation was not previously recognized (26). A striking and novel observation in the pulldown using phosphorylated peptide was the prominence of non-erythrocyte αII and βII spectrins (fodrins) and the spectrin-interacting proteins ankyrin and band 4.1B (27, 28). In addition, we saw two isoforms of cytoplasmic actin,

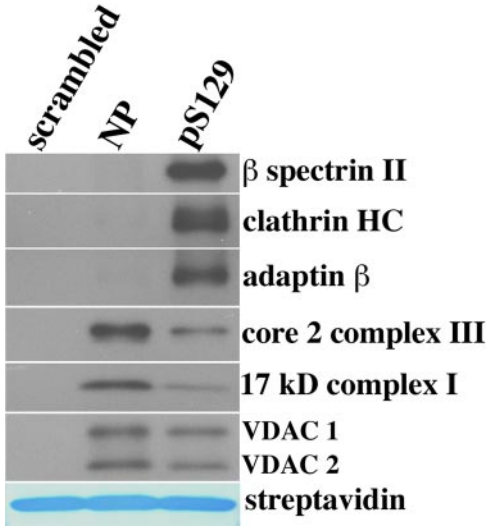

FIG. 3. **Composite of Western analyses confirming phosphorylation-dependent binding of selected human proteins.** Human brain proteins bind the carboxyl terminus of α-synuclein in a sequence- and phosphorylation-dependent manner. A composite of Western blots of total human synaptosomal protein pulled down by magnetic beads is shown. Each lane is labeled with the peptide bound to the magnetic beads that was used for each pulldown (scrambled, NP, and pS129). Pulldown experiments were performed as in Fig. 1. Eluted proteins bound to each peptide were separated by SDS-PAGE (4–20%), and Western analysis was performed with various antibodies as indicated to the *right* of the Western blots as described under "Experimental Procedures." *HC*, heavy chain.

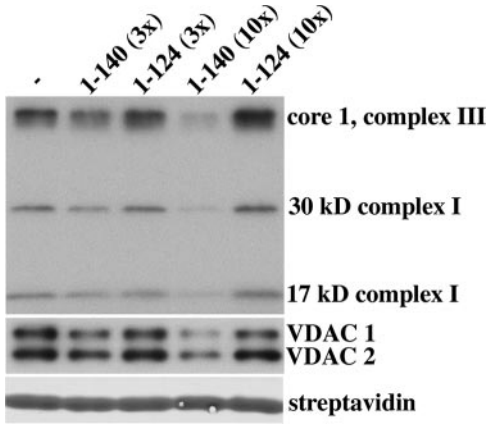

FIG. 4. **Competition with the NP peptide pulldown by full-length recombinant human α-synuclein.** Pulldown experiments using biotinylated NP peptide were performed in the presence or absence of a 3× or 10× molar excess of recombinant full-length human α-synuclein (residues 1–140) or a control protein consisting of truncated α-synuclein lacking the terminal 16 amino acids (residues 1–124). Eluted proteins bound to the biotinylated peptide were separated by SDS-PAGE (4–20%), and Western analysis was performed using specific antibodies. The eluted protein mixture was stained with GelCode Blue to identify the streptavidin, which served as a gel loading control.

β- and γ-actin (29, 30); non-muscle myosins; and one species of neurofilament. These proteins are present in the presynaptic portion of neurons and form what has been referred to as the presynaptic particle web involved in stabilization of the synapse (31, 40). This result suggests that phosphorylation could promote tethering of α-synuclein to the synaptic cytoskeleton, thereby also holding synaptic vesicles bound to the amino-terminal amphipathic helix of α-synuclein in place as well.

In Lewy bodies, α-synuclein is predominantly phosphorylated at Ser-129 (7). Lewy bodies have been shown to contain cytoskeletal proteins, including MAP1B, spectrin, cytoplasmic actin, neurofilament L, and tau (41). The data presented here suggest that the pathway to the production of Lewy bodies involves the interaction between phosphorylated α-synuclein and cytoskeletal elements.

Another interesting group of proteins interacting with phosphorylated α-synuclein are enzymes and signaling proteins involved in serine/threonine phosphorylation. Previous work has indicated that casein kinase 2 is the major kinase responsible for phosphorylation of α-synuclein at Ser-129 with much less activity demonstrated by casein kinase 1 and CaM kinase (12, 33). However, the increased affinity we saw for casein kinase 1, CaM kinase, and MARK2 with the phosphorylated peptide suggests either that these kinases are recognizing the product of phosphorylation rather than substrate or that they are not direct interactors with α-synuclein but are part of a complex that recognizes phosphorylated α-synuclein preferentially. It is worth noting, however, that the affinity of casein kinase 1 for phosphorylated α-synuclein is greater when the phosphorylation is at Tyr-125 rather than at Ser-129, raising the interesting possibility that Tyr-125 phosphorylation may be involved in a cooperative manner with serine phosphorylation at Ser-129. The tyrosine at position 125 can be phosphorylated by Src family kinases in cell culture, but we lack conclusive evidence that physiological phosphorylation at that site occurs in the brain (2, 3).

Clathrin heavy chain and subunits of AP-2 and AP-1 adapter complexes involved in clathrin-mediated endocytosis are also enriched among the proteins preferentially pulled down by phosphorylated α-synuclein over non-phosphorylated α-synuclein. AP-2 interacts with clathrin and is involved in endocytosis of synaptic vesicles destined to enter the recycling pool in the presynaptic region (42). If the interaction between the clathrin·AP-2 complex and α-synuclein is direct, this finding is of interest because recent data show that α-synuclein may be required for the genesis and/or maintenance of the "reserve" or "resting" pools of presynaptic vesicles (5–7). Proteins involved in vesicle trafficking were also identified as modifiers of α-synuclein toxicity in screens of *C. elegans* (8, 43). Thus, phosphorylation of α-synuclein may be important for its involvement in synaptic vesicle endocytosis.

There remains a long list of proteins showing a substantial preference for phosphorylated α-synuclein such as limbic system-associated membrane protein precursor, serine β-lactamase-like protein, and opioid-binding protein/cell adhesion molecule-like. Although it is impossible to group all of

these proteins into a coherent interaction network, our hope is that many of these proteins will serve as impetus for further experiments in the field.

Non-phosphorylated α-Synuclein Affinity—The pulldown using the NP peptide was enriched for a very different set of proteins than was found with either the pS129 or pY125 peptides (Table IV). The most striking finding is that the NP peptide pulled down a large number of subunits of electron transport chain proteins with much greater affinity than did either of the phosphorylated peptides. Table IV includes 31 of the 46 subunits of complex I of the electron transport chain as well as many complex III and complex IV proteins but not complex II proteins. Complex I is an L-shaped multimer with one hydrophobic arm that is inside the inner mitochondrial membrane and a more hydrophilic arm that is outside the membrane (45, 46). The 31 subunits of complex I listed in Table IV are not from any known precursor subcomplex of complex I and include proteins that seed complex I assembly, such as the mitochondrially encoded proteins, those that enter the complex somewhat later but prior to incorporation of the B17.2L chaperone, and proteins that come into the complex late and are located in the hydrophilic arm, such as NDUFS4 and NDUFS6 (45). A previous proteomics analysis of purified complex I showed that many of the complex III and IV proteins identified here co-purify as contaminants (47), reflecting the existence of a supercomplex consisting of complexes I, III, and IV referred to as the respirasome (35). Thus, we propose that the enrichment for electron transport chain proteins pulled down with the non-phosphorylated carboxyl terminus of α-synuclein is consistent with a preferential interaction of α-synuclein with one or more components of the respirasome complex.

There are a number of limitations to the study reported here. The first is that some of the proteins pulled down in a phosphorylation-dependent manner are likely false positives. Some are likely technical false positives due to nonspecific interactions with biotinylated peptide and the streptavidin beads. Based on the results with scrambled peptide, we believe this class of false positives is rather small. A larger class of false positives is made up of biological false positives. These proteins are likely to be in protein complexes in which only a small number of proteins are actually interacting, whereas the rest are pulled down through their association in the complex. Identifying which proteins are directly interacting will require substantial additional experiments to sort through these lists and test them for direct interaction. We have initiated such experiments using the yeast two-hybrid system to test for direct interactions and have already found domains in some of the cytoskeletal proteins in Table II that can interact directly with the carboxyl-terminal portion of α-synuclein.[2] A second limitation is that the experiments were performed with only a portion of α-synuclein. Although the competition experiment demonstrated that the COOH terminus when part of the full-length protein was able to specifically compete with a representative sample of the interactions, it still remains true that these experiments do not capture all the changes in conformation and subsequent interactions of the full-length protein conferred by phosphorylation. Finally the results described here are all derived from *in vitro* experiments, and the biological significance of many of these interactions remains an open question. Additional studies need to be performed in relevant living cells, such as neurons, in which the α-synuclein is either constitutively phosphorylated or is unphosphorylatable. The results reported here are only the first steps that should prove useful for generating novel hypotheses to be tested in more biologically complex and authentic systems.

There are a number of published proteomics studies describing interactions of α-synuclein with cellular proteins. These studies have primarily involved treating cells or whole animals with mitochondrial poisons, such as rotenone or 1-methyl-4-phenyl-1,2,5,6-tetrahydropyridine, and then performing a quantitative proteomics analysis of the changes in the identity and quantity of proteins found to interact with α-synuclein on an affinity column (48–50). To the best of our knowledge, ours is the first proteomics study to evaluate phosphorylation-dependent α-synuclein interactions. Fewer than a dozen proteins were found to overlap between these published studies and the research presented here. This may not be quite so surprising given that the previously published studies were designed to address different questions than the question being asked here. The published studies were looking for changes in proteins that interact with α-synuclein after toxic stress, whereas this study was designed to identify proteins with differential binding affinity for phosphorylated *versus* non-phosphorylated α-synuclein. None of the studies on proteins interacting with α-synuclein after exposure to toxins addressed the question of the phosphorylation status of α-synuclein in the treated *versus* untreated samples of cells or brain tissues. If there were little in the way of significant changes in the phosphorylation status of α-synuclein following these treatments, then we would not expect that the changes seen in those studies should overlap substantially with our data. If the bulk of α-synuclein remained non-phosphorylated after treatment with these toxins, an interaction with mitochondrial proteins would be missed because mitochondria were specifically excluded in two of these studies, whereas in the third there was substantial mitochondrial damage and cell loss.

Complex I dysfunction has long been hypothesized as an important component of the pathogenesis of PD (51–54). Li *et al.* (55) proposed that α-synuclein co-purifies with a mitochondrial fraction from brain and reported an immunogold electron micrograph showing a small number of gold particles marking the outer mitochondrial membrane using antibody against α-synuclein. In published results, we also demonstrated that α-synuclein, when expressed at low to moderate

[2] V. Drews and R. L. Nussbaum, unpublished data.

levels in stably transfected neuroblastoma cells, could translocate onto mitochondrial membranes following oxidative stress or reduced intracellular pH (56). This membrane interaction was likely through binding to cardiolipin, an acidic phospholipid for which the lipid binding amino-terminal portion of α-synuclein has high affinity, and no evidence was found for α-synuclein actually entering the mitochondria. The electron transport chain complexes are located within the inner mitochondrial membrane, however, and it is therefore puzzling to find a predominance of electron transport chain proteins pulled down by non-phosphorylated α-synuclein in the current study.

In contrast to our results (56), Devi *et al.* (57) and Parihar *et al.* (58) demonstrated that in cells that overexpressed α-synuclein the protein can enter mitochondria and interfere with mitochondrial function. Devi *et al.* (57) and Li *et al.* (55) went on to propose that the large number of lysines present in the repeated motifs in the amino terminus of the protein can serve as a cryptic mitochondrial targeting sequence that allows α-synuclein to enter mitochondria. One can hypothesize that with high levels of expression of non-phosphorylated α-synuclein the protein is untethered to cytoskeletal elements and is free to enter mitochondria where it can interfere with complex I of the electron transport chain. If perhaps the capacity to phosphorylate α-synuclein is limiting, overexpression of the protein or mutations that prolong its half-life would increase the levels of non-phosphorylated protein disproportionately and, therefore, cause more mitochondrial inhibition. These results are consistent with the results of Gorbatyuk *et al.* (16) and support a model that places non-phosphorylated α-synuclein in the pathway leading to mitochondrial dysfunction and the development of PD. The enzymes involved in phosphorylating and dephosphorylating α-synuclein might, therefore, be potential therapeutic targets in PD.

Acknowledgments—We thank Douglas Slotta, Sara Yang, and Anthony J. Makusky for help with data processing; Jeffrey Kowalak and Joanne Connolly for preliminary observations on this project; and Dr. Yien-Ming Kuo and Dr. Valerie Drews for help in preparing and critically reading the manuscript. We thank Nelson Cole for providing some recombinant synucleins and helping us to make others.

* This work was supported, in whole or in part, by National Institutes of Health Grant Z01 MH000279 from the intramural programs of the National Institute of Mental Health and by the NHGRI. This work was also supported by the Sandler Family Foundation. The costs of publication of this article were defrayed in part by the payment of page charges. This article must therefore be hereby marked "*advertisement*" in accordance with 18 U.S.C. Section 1734 solely to indicate this fact.

S The on-line version of this article (available at http://www.mcponline.org) contains supplemental material.

§ Both authors contributed equally to this work.

** To whom correspondence should be addressed: Division of Medical Genetics, University of California, Box 0794, 513 Parnassus Ave., Rm. HSE901E, San Francisco, CA 94143-0794. Tel.: 415-476-3200; Fax: 415-476-1356; E-mail: nussbaumr@humgen.ucsf.edu.

REFERENCES

1. George, J. M. (2002) The synucleins. *Genome Biol.* **3,** REVIEWS3002
2. Beal, M. F. (2001) Experimental models of Parkinson's disease. *Nat. Rev. Neurosci.* **2,** 325–334
3. Bennett, M. C. (2005) The role of α-synuclein in neurodegenerative diseases. *Pharmacol. Ther.* **105,** 311–331
4. Larsen, K. E., Schmitz, Y., Troyer, M. D., Mosharov, E., Dietrich, P., Quazi, A. Z., Savalle, M., Nemani, V., Chaudhry, F. A., Edwards, R. H., Stefanis, L., and Sulzer, D. (2006) α-Synuclein overexpression in PC12 and chromaffin cells impairs catecholamine release by interfering with a late step in exocytosis. *J. Neurosci.* **26,** 11915–11922
5. Murphy, D. D., Rueter, S. M., Trojanowski, J. Q., and Lee, V. M. (2000) Synucleins are developmentally expressed, and α-synuclein regulates the size of the presynaptic vesicular pool in primary hippocampal neurons. *J. Neurosci.* **20,** 3214–3220
6. Cabin, D. E., Shimazu, K., Murphy, D., Cole, N. B., Gottschalk, W., McIlwain, K. L., Orrison, B., Chen, A., Ellis, C. E., Paylor, R., Lu, B., and Nussbaum, R. L. (2002) Synaptic vesicle depletion correlates with attenuated synaptic responses to prolonged repetitive stimulation in mice lacking α-synuclein. *J. Neurosci.* **22,** 8797–8807
7. Gureviciene, I., Gurevicius, K., and Tanila, H. (2007) Role of α-synuclein in synaptic glutamate release. *Neurobiol. Dis.* **28,** 83–89
8. Cooper, A. A., Gitler, A. D., Cashikar, A., Haynes, C. M., Hill, K. J., Bhullar, B., Liu, K., Xu, K., Strathearn, K. E., Liu, F., Cao, S., Caldwell, K. A., Caldwell, G. A., Marsischky, G., Kolodner, R. D., Labaer, J., Rochet, J. C., Bonini, N. M., and Lindquist, S. (2006) α-Synuclein blocks ER-Golgi traffic and Rab1 rescues neuron loss in Parkinson's models. *Science* **313,** 324–328
9. Kuwahara, T., Koyama, A., Koyama, S., Yoshina, S., Ren, C. H., Kato, T., Mitani, S., and Iwatsubo, T. (2008) A systematic RNAi screen reveals involvement of endocytic pathway in neuronal dysfunction in α-synuclein transgenic C. elegans. *Hum. Mol. Genet*., in press
10. Ellis, C. E., Schwartzberg, P. L., Grider, T. L., Fink, D. W., and Nussbaum, R. L. (2001) α-Synuclein is phosphorylated by members of the Src family of protein-tyrosine kinases. *J. Biol. Chem.* **276,** 3879–3884
11. Nakamura, T., Yamashita, H., Takahashi, T., and Nakamura, S. (2001) Activated Fyn phosphorylates α-synuclein at tyrosine residue 125. *Biochem. Biophys. Res. Commun.* **280,** 1085–1092
12. Okochi, M., Walter, J., Koyama, A., Nakajo, S., Baba, M., Iwatsubo, T., Meijer, L., Kahle, P. J., and Haass, C. (2000) Constitutive phosphorylation of the Parkinson's disease associated α-synuclein. *J. Biol. Chem.* **275,** 390–397
13. Anderson, J. P., Walker, D. E., Goldstein, J. M., de Laat, R., Banducci, K., Caccavello, R. J., Barbour, R., Huang, J. P., Kling, K., Lee, M., Diep, L., Keim, P. S., Shen, X. F., Chataway, T., Schlossmacher, M. G., Seubert, P., Schenk, D., Sinha, S., Gai, W. P., and Chilcote, T. J. (2006) Phosphorylation of Ser-129 is the dominant pathological modification of α-synuclein in familial and sporadic Lewy body disease. *J. Biol. Chem.* **281,** 29739–29752
14. Fujiwara, H., Hasegawa, M., Dohmae, N., Kawashima, A., Masliah, E., Goldberg, M. S., Shen, J., Takio, K., and Iwatsubo, T. (2002) α-Synuclein is phosphorylated in synucleinopathy lesions. *Nat. Cell Biol.* **4,** 160–164
15. Mattei, M. G., Mattei, J. F., Vidal, I., and Giraud, F. (1981) Expression in lymphocyte and fibroblast culture of the fragile-X chromosome: a new technical approach. *Hum. Genet.* **59,** 166–169
16. Gorbatyuk, O. S., Li, S., Sullivan, L. F., Chen, W., Kondrikova, G., Manfredsson, F. P., Mandel, R. J., and Muzyczka, N. (2008) The phosphorylation state of Ser-129 in human α-synuclein determines neurodegeneration in a rat model of Parkinson disease. *Proc. Natl. Acad. Sci.* U.S.A. **105,** 763–768
17. Ellis, C. E., Murphy, E. J., Mitchell, D. C., Golovko, M. Y., Scaglia, F., Barcelo-Coblijn, G. C., and Nussbaum, R. L. (2005) Mitochondrial lipid abnormality and electron transport chain impairment in mice lacking α-synuclein. *Mol. Cell. Biol.* **25,** 10190–10201
18. Shevchenko, A., Wilm, M., Vorm, O., and Mann, M. (1996) Mass spectrometric sequencing of proteins from silver stained polyacrylamide gels. *Anal. Chem.* **68,** 850–858
19. Masuda, J., Maynard, D. A., Nishimura, M., Uedac, T., Kowalak, J. A., and Markey, S. P. (2005) Fully automated micro- and nanoscale one- or two-dimensional high-performance liquid chromatography system for liquid chromatography-mass spectrometry compatible with non-volatile

salts for ion exchange chromatography. *J. Chromatogr. A* **1063,** 57–69
20. Slotta, D. J., McFarland, M. A., Makusky, S. J., and Markey, S. P. (2007) in the *55th ASMS Conference on Mass Spectrometry and Allied Topics, Indianapolis, June 3–7, 2007*, Abstract 157, American Society for Mass Spectrometry, Santa Fe, NM
21. Yang, X. Y., Dondeti, V., Dezube, R., Maynard, D. M., Geer, L. Y., Epstein, J., Chen, X. F., Markey, S. P., and Kowalak, J. A. (2004) DBParser: Web-based software for shotgun proteomic data analyses. *J. Proteome Res.* **3,** 1002–1008
22. Dosemeci, A., Makusky, A. J., Jankowska-Stephens, E., Yang, X., Slotta, D. J., and Markey, S. P. (2007) Composition of the synaptic PSD-95 complex. *Mol. Cell. Proteomics* **6,** 1749–1760
23. McFarland, M. A., Yang, X., Geer, L. Y., Makusky, A. J., Kowalak, J. A., Nussbaum, R. L., and Markey, S. P. (2006) in the *54th ASMS Conference on Mass Spectrometry and Allied Topics, Seattle, May 28–June 1, 2006*, Abstract 584, American Society for Mass Spectrometry, Santa Fe, NM
24. Florens, L., Carozza, M. J., Swanson, S. K., Fournier, M., Coleman, M. K., Workman, J. L., and Washburn, M. P. (2006) Analyzing chromatin remodeling complexes using shotgun proteomics and normalized spectral abundance factors. *Methods* **40,** 303–311
25. Paoletti, A. C., Parmely, T. J., Tomomori-Sato, C., Sato, S., Zhu, D. X., Conaway, R. C., Conaway, J. W., Florens, L., and Washburn, M. P. (2006) Quantitative proteomic analysis of distinct mammalian Mediator complexes using normalized spectral abundance factors. *Proc. Natl. Acad. Sci. U. S. A.* **103,** 18928–18933
26. Jensen, P. H., Islam, K., Kenney, J., Nielsen, M. S., Power, J., and Gai, W. P. (2000) Microtubule-associated protein 1B is a component of cortical Lewy bodies and binds α-synuclein filaments. *J. Biol. Chem.* **275,** 21500–21507
27. Bennett, V., Baines, A. J., and Davis, J. Q. (1985) Ankyrin and synapsin: spectrin-binding proteins associated with brain membranes. *J. Cell. Biochem.* **29,** 157–169
28. Bennett, V., Baines, A. J., and Davis, J. (1986) Purification of brain analogs of red blood cell membrane skeletal proteins: ankyrin, protein 4.1 (synapsin), spectrin, and spectrin subunits. *Methods Enzymol.* **134,** 55–69
29. Vandekerckhove, J., and Weber, K. (1978) Mammalian cytoplasmic actins are the products of at least two genes and differ in primary structure in at least 25 identified positions from skeletal muscle actins. *Proc. Natl. Acad. Sci. U. S. A.* **75,** 1106–1110
30. Garrels, J. I., and Gibson, W. (1976) Identification and characterization of multiple forms of actin. *Cell* **9,** 793–805
31. Phillips, G. R., Huang, J. K., Wang, Y., Tanaka, H., Shapiro, L., Zhang, W., Shan, W. S., Arndt, K., Frank, M., Gordon, R. E., Gawinowicz, M. A., Zhao, Y., and Colman, D. R. (2001) The presynaptic particle web: ultrastructure, composition, dissolution, and reconstitution. *Neuron* **32,** 63–77
32. Voglmaier, S. M., and Edwards, R. H. (2007) Do different endocytic pathways make different synaptic vesicles? *Curr. Opin. Neurobiol.* **17,** 374–380
33. Ishii, A., Nonaka, T., Taniguchi, S., Saito, T., Arai, T., Mann, D., Iwatsubo, T., Hisanaga, S., Goedert, M., and Hasegawa, M. (2007) Casein kinase 2 is the major enzyme in brain that phosphorylates Ser129 of human α-synuclein: implication for α-synucleinopathies. *FEBS Lett.* **581,** 4711–4717
34. Ostrerova, N., Petrucelli, L., Farrer, M., Mehta, N., Choi, P., Hardy, J., and Wolozin, B. (1999) α-Synuclein shares physical and functional homology with 14-3-3 proteins. *J. Neurosci.* **19,** 5782–5791
35. Schagger, H., de Coo, R., Bauer, M. F., Hofmann, S., Godinot, C., and Brandt, U. (2004) Significance of respirasomes for the assembly/stability of human respiratory chain complex I. *J. Biol. Chem.* **279,** 36349–36353
36. Nakajo, S., Tsukada, K., Omata, K., Nakamura, Y., and Nakaya, K. (1993) A new brain-specific 14-kDa protein is a phosphoprotein. Its complete amino acid sequence and evidence for phosphorylation. *Eur. J. Biochem.* **217,** 1057–1063
37. Lavedan, C. (1998) The synuclein family. *Genome Res.* **8,** 871–880
38. Mueller, L., Brusniak, M., Mani, D., and Aebersold, R. (2008) An assessment of software solutions for the analysis of mass spectrometry based quantitative proteomics data. *J. Proteome Res.* **1,** 51–61
39. Ong, S. E., and Mann, M. (2005) Mass spectrometry-based proteomics turns quantitative. *Nat. Chem. Biol.* **1,** 252–262
40. Pielage, J., Fetter, R. D., and Davis, G. W. (2005) Presynaptic spectrin is essential for synapse stabilization. *Curr. Biol.* **15,** 918–928
41. Leverenz, J. B., Umar, I., Wang, Q., Montine, T. J., McMillan, P. J., Tsuang, D. W., Jin, J. H., Pan, C., Shin, J., Zhu, D., and Zhang, J. (2007) Proteomic identification of novel proteins in cortical Lewy bodies. *Brain Pathol.* **17,** 139–145
42. Knoll, J. H., Chudley, A. E., and Gerrard, J. W. (1984) Fragile-X X-linked mental retardation II. Frequency and replication pattern of fragile (X)(q28) in heterozygotes. *Am. J. Hum. Genet.* **36,** 640–645
43. van Ham, T. J., Thijssen, K. L., Breitling, R., Hofstra, R. M., Plasterk, R. H., and Nollen, E. A. (2008) C. elegans model identifies genetic modifiers of α-synuclein inclusion formation during aging. *PLoS Genet.* **4,** e1000027
44. Thomas, B., and Beal, M. F. (2007) Parkinson's disease. *Hum. Mol. Genet.* **16,** R183–R194
45. Lazarou, M., McKenzie, M., Ohtake, A., Thorburn, D. R., and Ryan, M. T. (2007) Analysis of the assembly profiles for mitochondrial- and nuclear-DNA-encoded subunits into complex I. *Mol. Cell. Biol.* **27,** 4228–4237
46. McKenzie, M., Lazarou, M., Thorburn, D. R., and Ryan, M. T. (2007) Analysis of mitochondrial subunit assembly into respiratory chain complexes using Blue Native polyacrylamide gel electrophoresis. *Anal. Biochem.* **364,** 128–137
47. Pocsfalvi, G., Cuccurullo, M., Schlosser, G., Cacace, G., Siciliano, R. A., Mazzeo, M. F., Scacco, S., Cocco, T., Gnoni, A., Malorni, A., and Papa, S. (2006) Shotgun proteomics for the characterization of subunit composition of mitochondrial complex I. *Biochim. Biophys. Acta* **1757,** 1438–1450
48. Zhou, Y., Gu, G., Goodlett, D. R., Zhang, T., Pan, C., Montine, T. J., Montine, K. S., Aebersold, R. H., and Zhang, J. (2004) Analysis of α-synuclein-associated proteins by quantitative proteomics. *J. Biol. Chem.* **279,** 39155–39164
49. Jin, J., Li, G. J., Davis, J., Zhu, D., Wang, Y., Pan, C., and Zhang, J. (2007) Identification of novel proteins associated with both α-synuclein and DJ-1. *Mol. Cell. Proteomics* **6,** 845–859
50. Jin, J. H., Meredith, G. E., Chen, L., Zhou, Y., Xu, J., Shie, F. S., Lockhart, P., and Zhang, J. (2005) Quantitative proteomic analysis of mitochondrial proteins: relevance to Lewy body formation and Parkinson's disease. *Mol. Brain Res.* **134,** 119–138
51. Greenamyre, J. T., Sherer, T. B., Betarbet, R., and Panov, A. V. (2001) Complex I and Parkinson's disease. *IUBMB Life* **52,** 135–141
52. Hanagasi, H. A., Ayribas, D., Baysal, K., and Emre, M. (2005) Mitochondrial complex I, II/III, and IV activities in familial and sporadic Parkinson's disease. *Int. J. Neurosci.* **115,** 479–493
53. Song, D. D., Shults, C. W., Sisk, A., Rockenstein, E., and Masliah, E. (2004) Enhanced substantia nigra mitochondrial pathology in human α-synuclein transgenic mice after treatment with MPTP. *Exp. Neurol.* **186,** 158–172
54. Fornai, F., Schluter, O. M., Lenzi, P., Gesi, M., Ruffoli, R., Ferrucci, M., Lazzeri, G., Busceti, C. L., Pontarelli, F., Battaglia, G., Pellegrini, A., Nicoletti, F., Ruggieri, S., Paparelli, A., and Sudhof, T. C. (2005) Parkinson-like syndrome induced by continuous MPTP infusion: convergent roles of the ubiquitin-proteasome system and α-synuclein. *Proc. Natl. Acad. Sci. U. S. A.* **102,** 3413–3418
55. Li, W. W., Yang, R., Guo, J. C., Ren, H. M., Zha, X. L., Cheng, J. S., and Cai, D. F. (2007) Localization of α-synuclein to mitochondria within midbrain of mice. *Neuroreport* **18,** 1543–1546
56. Cole, N. B., Dieuliis, D., Leo, P., Mitchell, D. C., and Nussbaum, R. L. (2008) Mitochondrial translocation of α-synuclein is promoted by intracellular acidification. *Exp. Cell Res.* **314,** 2076–2089
57. Devi, L., Raghavendran, V., Prabhu, B. M., Avadhani, N. G., and Anandatheerthavarada, H. K. (2008) Mitochondrial import and accumulation of α-synuclein impair complex I in human dopaminergic neuronal cultures and Parkinson disease brain. *J. Biol. Chem.* **283,** 9089–9100
58. Parihar, M. S., Parihar, A., Fujita, M., Hashimoto, M., and Ghafourifar, P. (2008) Mitochondrial association of α-synuclein causes oxidative stress. *CMLS Cell. Mol. Life Sci.* **65,** 1272–1284